AEM
Journals.ASM.org

Mechanism of the Synergistic Inactivation of *Escherichia coli* by UV-C Light at Mild Temperatures

E. Gayán, P. Mañas, I. Álvarez, S. Condón

Food Technology, Faculty of Veterinary, University of Zaragoza, Zaragoza, Spain

UV light only penetrates liquid food surfaces to a very short depth, thereby limiting its industrial application in food pasteurization. One promising alternative is the combination of UV light with mild heat (UV-H), which has been demonstrated to produce a synergistic bactericidal effect. The aim of this article is to elucidate the mechanism of synergistic cellular inactivation resulting from the simultaneous application of UV light and heat. The lethality of UV-H treatments remained constant below ~45°C, while lethality increased exponentially as the temperature increased. The percentage of synergism reached a maximum (40.3%) at 55°C. Neither the flow regimen nor changes in the dose delivered by UV lamps contributed to the observed synergism. UV-H inactivation curves of the parental *Escherichia coli* strain obtained in a caffeic acid selective recovery medium followed a similar profile to those obtained with *uvrA* mutant cells in a nonselective medium. Thermal fluidification of membranes and synergistic lethal effects started around 40 to 45°C. Chemical membrane fluidification with benzyl alcohol decreased the UV resistance of the parental strain but not that of the *uvrA* mutant. These results suggest that the synergistic lethal effect of UV-H treatments is due to the inhibition of DNA excision repair resulting from the membrane fluidification caused by simultaneous heating.

UV-C light is an emerging disinfection technology for water and, more recently, for liquid foods due to its multiple advantages (1, 2). UV-C (220 to 300 nm) has a germicidal effect for most types of microorganisms because it produces photochemical modifications of nucleic acids' pyrimidine bases. The major UV-induced DNA lesion is cyclobutane pyrimidine dimers (CPDs), while (6-4) photoproducts (6-4PPs) are also formed on about 25% of CPDs (3). These lesions prevent the proper replication and transcription of DNA, resulting in mutagenesis and, ultimately, cell death (4). The magnitude of the lethal effect depends on the radiation dose and on the cells' ability to repair damage.

Microorganisms have adopted various enzymatic DNA repair pathways to restore DNA molecules from replication errors and the action of both endogenous and exogenous DNA-damaging agents. The DNA repair pathways involved in damage repair prior to replication include photorepair, base excision repair (BER), and nucleotide excision repair (NER) (3, 4). Under extensive DNA damage, repair mechanisms controlled by the SOS regulon, such as RecA-mediated excision repair (RAMER), translesion synthesis (TLS), and homologous recombination (HR) repair, are induced (4, 5). Overall, the lethality of UV light could be improved by impairing bacterial DNA repair mechanisms.

The ability of UV light to be used for liquid food hygienization has been widely demonstrated (2, 6). In fact, UV-based technologies have been approved as alternative treatments to thermal pasteurization of fresh juice products (7). However, the implementation of UV processing in the food industry is still limited due to the large amounts of UV-absorbing compounds and suspended particles of foods, which reduce UV light transmittance into liquids, thereby preventing the ability to achieve significant microbial inactivation. To overcome this limitation, new processes have been designed by combining several technologies applied at lower intensities, but with equivalent or even higher degrees of stability and safety. The interactions of UV light applied simultaneously with chemical agents (8, 9, 10) and with different energies, such as ionizing radiation (11) and heat (12–14), have been reported. Regarding the latter, there is an increased interest in the potential use of UV light combined with mild heat (UV-H treatments) for pasteurization of high-UV-absorptivity liquid foods (15), as this combination has been demonstrated to have a synergistic lethal effect on *Escherichia coli* (12) and *Salmonella enterica* subsp. *enterica* serovar Typhimurium (16) at temperatures around 50 to 60°C. Petin et al. (14) suggested two possible explanations for the synergistic lethal effect of the combined process, which are not contradictory: the reduction of cellular capacity to repair DNA damage by thermal effects and the interaction of sublethal lesions induced by each of the agents. Despite being of interest, the mechanism of microbial killing improvement by UV light in combination with mild heat is not known.

The aim of this article is to elucidate the mechanism of synergistic cellular inactivation by the simultaneous application of UV light and heat. For this purpose, we evaluated changes in the effective dose either by changes in the flow pattern or UV lamps' efficiency to discard the effect of physical factors, and in a second step, we studied the biological basis of the synergistic effect. The *E. coli* K-12 strain was selected as a model microorganism.

MATERIALS AND METHODS

Bacterial culture. *Escherichia coli* K-12 substrain BW25113 and its isogenic deletion mutants, listed in Table 1, were obtained from the Keio collection (17). The bacterial cultures were kept frozen at −80°C in cryovials. Stationary-phase cultures were prepared by inoculation of 10 ml of tryptone soy broth (Biolife, Milan, Italy) supplemented with 0.6% (wt/vol) yeast extract (Biolife) (TSBYE) with a loopful of growth from tryptone soy agar (Biolife) supplemented with 0.6% (wt/vol) yeast extract (TSAYE). The cultures were incubated at 35°C for 6 h in a shaking incubator. Fifty microliters of the cultures was inoculated into 50 ml of fresh

Received 26 February 2013 Accepted 12 May 2013
Published ahead of print 17 May 2013
Address correspondence to Santiago Condón, scondon@unizar.es.
Copyright © 2013, American Society for Microbiology. All Rights Reserved.
doi:10.1128/AEM.00623-13

TABLE 1 *E. coli* BW25113 derivatives used in this investigation with different DNA repair pathways deleted

Derivative	Relevant genotype	Description	DNA repair mechanisms affected
JW0698	Δ*phr-758*::*kan*	Deoxyribodipyrimidine photolyase	Photoreactivation
JW1625	Δ*nth-782*::*kan*	Thymine glycol-DNA glycosylase (TG-DNA glycosylase) or endonuclease III	Base excision repair
JW4019	Δ*uvrA753*::*kan*	ATPase and DNA damage recognition protein of nucleotide excision repair excinuclease UvrABC	Nucleotide excision repair
JW1172	Δ*umuD772*::*kan*	Subunit D of DNA polymerase V	Translesion synthesis
JW2669	Δ*recA774*::*kan*	DNA strand exchange and recombination protein with protease and nuclease activity	SOS response: RecA-mediated excision repair, translesion synthesis, and homologous recombination repair

TSBYE and incubated for 24 h under the same conditions, which resulted in stationary-phase cultures containing ~10^9 CFU ml^{-1}. All media were sterilized at 121°C for 20 min.

UV treatments. The UV equipment used in this investigation was previously described by Gayán et al. (12). The entire system was formed by eight annular thin-film flowthrough reactors connected in series with a sampling valve at the exit of each reactor. Each reactor consisted of a low-pressure UV lamp (TUV 8WT5; Philips) with an input power of 8 W (85% of energy emitted at a wavelength of 254 nm) enclosed by a quartz tube. The annular gap between the quartz tube and the outside glass sleeve, where liquid flowed, was 2.5 mm. The reactors were submerged in a tempered 90-liter water bath (temperature [T] ± 1.5°C) heated by the circulating water of a peripheral thermostatic bath (model Kattebad K12; Huber, Offenburg, Germany). Two thermocouples (model ZA 020-FS; Almeco, Bernburg, Germany) located at the input of the first reactor and the outlet of the last reactor allowed the treatment temperature to be controlled.

The treatment medium was added with the bacterial suspension to achieve ~10^7 CFU ml^{-1} and pumped (8.5 liters h^{-1}) through the heat exchanger to the reactors. When the treatment conditions were stabilized, samples were withdrawn through the sampling valves at the outlet of each reactor, and 0.1 or 1 ml was immediately pour plated in the recovery media. A sterile McIlvaine citrate-phosphate buffer of pH 7.0 (18) with an absorption coefficient of 23.6 cm^{-1}, close to that of clarified apple juice, was used as the UV-H treatment medium. To compare the resistance and the inactivation kinetics of *E. coli* derivatives to UV light at room temperature, McIlvaine buffer of pH 7.0 with a lower absorption coefficient (15.3 cm^{-1}) was used. Buffers of different absorption coefficients were prepared by adding after buffer sterilization different quantities of tartrazine (Sigma-Aldrich, St. Louis, MO) and adjusting the medium absorbance to 254 nm using a Unicam UV500 spectrophotometer (Unicam Limited, Cambridge, United Kingdom) as described by Gayán et al. (12). Prior to and following each treatment session, the UV equipment was cleaned and sanitized using an ethanol solution (Aldipa, Zaragoza, Spain) (30% [vol/vol]) and rinsed with sterile distilled water with UV lamps on. Plating samples of the rinse water were checked to make sure they did not show microbial growth.

Heat treatments. Heat treatments were carried out in a specially designed resistometer (19). Briefly, this instrument consists of a 350-ml vessel equipped with an electrical heater for a thermostation, an agitation device to ensure inoculum distribution and temperature homogeneity, and ports for injecting the microbial suspension and for sample extraction. Once the preset temperature had attained stability (T ± 0.05°C), 0.2 ml of an adequately diluted microbial cell suspension were inoculated into the corresponding treatment medium. After inoculation, 0.2-ml samples were collected at different heating times and immediately pour plated. Prior to and following each treatment session, the vessel was sterilized at 121°C for 20 min.

Incubation of treated samples and survival counting. TSAYE was used as the recovery medium. Where indicated, the maximum noninhibitory concentration (MNIC) of caffeic acid (CA) (TSAYE-CA) (Panreac, Barcelona, Spain) was added to the recovery medium before it was sterilized to estimate the percentage of sublethally injured cells. The MNIC of caffeic acid (3.75 mg ml^{-1}) was chosen in previous experiments with nontreated cells (data not shown). The presence of caffeic acid in the recovery medium inhibits nucleotide excision repair by affecting UvrABC excinuclease activity (20, 21). Samples recovered in the nonselective medium were incubated for 24 h at 35°C, and those recovered in caffeic acid-enriched medium were incubated for 48 h at 35°C. Previous experiments demonstrated that longer incubation times did not change the profile of survival curves. After incubation, CFU were counted with an improved image analyzer automatic colony counter (Protos; Synoptics, Cambridge, United Kingdom), as described previously (22). For photoreactivation, 20 μl of different dilutions of each sample was spread plated in TSAYE-containing petri dishes under 13-W daylight fluorescent lamps (T16 13W/827-EVG, G5; Osram, Munich, Germany) that emitted light in the 360- to 700-nm-wavelength range. The distance between the surface of the test suspension and the lamp was 10 cm. The mean illuminance was 11.15 klx, and photoreactivation was performed for 60 min at 20°C. Previously, longer incubation times and higher temperatures were demonstrated to not improve survival counts. In each experiment, a sample of UV-irradiated suspension was kept in the dark under the same conditions as a reference. After photoreactivation, the plates were incubated for 24 h at 35°C.

Curve fitting, resistance parameters, and synergistic effect calculation. Survival curves to UV treatments were obtained by plotting the logarithm of the survival fraction versus treatment doses, expressed in energy consumption units (J ml^{-1}) for UV treatments at room temperature or time in min for heat and UV-H treatments. To fit survival curves and calculate resistance parameters, the Geeraerd and Van Impe inactivation model-fitting tool (GInaFiT) was used (23). Because our survival curves did not show tails but rather shoulders, the log-linear regression-plus-shoulder model (24) was used. This model describes the survival curves through two parameters: shoulder length (*Sl*), or time before the exponential inactivation begins, and the inactivation rate (K_{max}), defined as the slope of the exponential portion of the survival curve. For comparison purposes, the GInaFiT also provides the parameter 4*D*, defined as the treatment time necessary to inactivate 99.99% of the microbial population.

To determine the magnitude of the synergistic lethal effect of the combined UV-H treatment at each temperature, 4*D* values obtained experimentally (experimental $4D_{UV\text{-}H}$) were compared with theoretical $4D_{UV\text{-}H}$ values (time to achieve a 99.99% reduction in the microbial inactivation if the two processes act simultaneously but independently) calculated via the following equations proposed by Gayán et al. (15):

$$\text{theoretical } 4D_{UV\text{-}H} = \frac{(4D_H \times 4D_{UV})}{(4D_H + 4D_{UV})} \quad (1)$$

$$\%\ \text{synergism} = \frac{\text{theoretical } 4D_{UV\text{-}H} - \text{experimental } 4D_{UV\text{-}H}}{\text{theoretical } 4D_{UV\text{-}H}} \times 100 \quad (2)$$

where $4D_H$, and $4D_{UV}$ values were obtained from the fitting of the inactivation curves to heat and UV light, respectively.

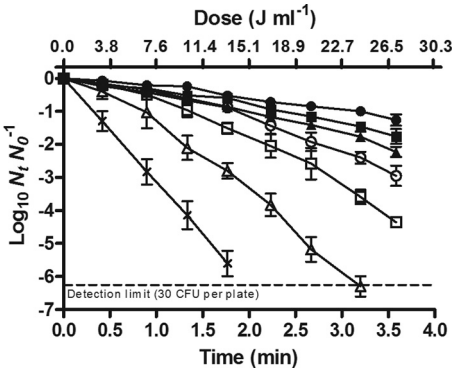

FIG 1 Survival curves of the *E. coli* WT strain treated by UV light at different temperatures: 25.0°C (●), 40.0°C (■), 50.0°C (▲), 52.5°C (○), 55.0°C (□), 57.5°C (△), and 60°C (X). Treatments were carried out in McIlvaine buffer with an absorption coefficient of 23.6 cm^{-1}, and survivors were recovered in the nonselective medium.

Membrane fluidity measurement. Fluorescence anisotropy was measured using diphenyl-1,3,5-hetratriene (DPH) (Sigma-Aldrich, Steinheim, Germany) as a lipophilic marker by a procedure similar to that described by Almeida et al. (25) and calculated according to Chu-Ky et al. (26). Fluorescence measurements were carried out in a Cary-Eclipse spectrofluorometer (Varian Medical Systems, Belrose, Australia) equipped with a manual fluorescence polarizer (Varian Medical Systems). The spectrofluorometer system contains four sample chambers that can be thermostated by an auxiliary thermostatic bath (Digiterm 3000613; Selecta SA, Barcelona, Spain). One milliliter of cell suspension was centrifuged (10,000 *g* for 5 min) and resuspended at a concentration of 10^8 CFU ml^{-1} in McIlvaine buffer (pH 7.0) with 0.25% (vol/vol) formaldehyde (Panreac). The obtained suspension was incubated with a solution of DPH in tetrahydrofuran (Scharlau, Barcelona, Spain) for 45 min at 35°C. To determine the fluorescence anisotropy at different temperatures (25 to 60°C), fluorescence measurements were performed after maintaining cells for 3.5 min at the preset temperature. The excitation and emission wavelengths used were 355 ± 5 nm and 425 nm ± 5 nm, respectively.

To evaluate the effect of cell membrane fluidity on the UV resistance at room temperature, cells were preincubated (20 min) and treated in the McIlvaine buffer with benzyl alcohol (BA) (Panreac, Barcelona, Spain) added at a concentration of 20 mM.

RTD distribution and delivered dose. The stimulus-response technique by impulsion was used for experimental determination of residence time distribution (RTD) curves, as previously described by Koutchma and Parisi (27), using saturated sodium chloride solution as a tracer. When the McIlvaine buffer flow achieved a steady-state condition (flow rate, 8.5 liters h^{-1}), 3 ml of the solution was injected with a syringe into the center of the pipe 3 cm before of the input of the UV reactor. The conductivity (Crison Instruments, Barcelona, Spain) of the output flow of the entire installation was measured as a function of time after injection. The sodium chloride concentration distribution [$c(t)$] curve was normalized to obtain the $E(t)$ curve (equation 3), from which the mean residence time ($\bar{t}$; equation 4) was calculated, as well as the variance (σ^2; equation 5) as a measure of the residence time dispersion:

$$E(t) = \frac{C(t)}{\int_0^t c(t)dt} \quad (3)$$

$$\bar{t} = \int_0^t tE(t)\,dt \quad (4)$$

$$\sigma^2 = \int_0^t t^2 E(t)dt - t^{-2} \quad (5)$$

The chemical quantification of the delivered UV intensity was performed with the iodide-iodate actinometer containing 0.6 M potassium iodide and 0.1 M potassium iodate in 0.01 M $Na_2B_4O_7 \cdot 12H_2O$ at pH 9.25 (Panreac, Barcelona, Spain). Determination of photoproduct I_3^- was carried out spectrophotochemically using an extinction coefficient of $\varepsilon_{352} = 27.60\ M^{-1}\ cm^{-1}$.

Statistical analysis. Statistical analyses, the *t* test ($P = 0.05$), and analysis of variance (ANOVA) ($P = 0.05$) were carried out using GraphPad PRISM 5.0 software (GraphPad Software, Inc., San Diego, CA), and differences were considered significant at $P \leq 0.05$. All microbial resistance determinations and analytical assays were performed at least three times on different working days. The error bars in the figures correspond to the mean standard deviation.

RESULTS

Synergistic lethal effect of UV-H treatments on *E. coli* wild-type inactivation. Figure 1 shows the survival curves of the *E. coli* wild type (WT) treated by UV light at different temperatures (25.0 to 60.0°C) in a McIlvaine buffer with an absorption coefficient of 23.6 cm^{-1} and recovered in a nonselective medium. As observed in the figure, the survival curves showed an initial lag phase followed by an exponential inactivation rate. Concave downward survival curves were fitted with the log-linear regression-plus-shoulder model described by Geeraerd et al. (24). Estimated parameters of the model (*Sl* and K_{max}) and 4*D* values are compiled in Table 2. The table includes the coefficient of determination (R^2) and the root mean square error (RMSE) values obtained from the

TABLE 2 Resistance parameters obtained from the fitting of Geeraerd et al.'s model to the survival curves of the *E. coli* WT and the *uvrA* isogenic mutant[a]

	Wild-type strain										*uvrA* mutant (TSAYE)				
	TSAYE					TSAYE-CA									
Temp (°C)	*Sl* (min)	K_{max} (min^{-1})	4*D* (min)	R^2	RMSE	*Sl* (min)	K_{max} (min^{-1})	4*D* (min)	R^2	RMSE	*Sl* (min)	K_{max} (min^{-1})	4*D* (min)	R^2	RMSE
25.0	0.96 (0.07) A	1.13 (0.23) A	9.07 (0.43) A	0.958	0.116	0 B	3.63 (0.25) B	2.56 (0.13) B	0.960	0.501	0 B	3.79 (0.56) B	2.37 (0.12) B	0.985	0.260
40.0	0.91 (0.03) A	1.38 (0.31) A	7.57 (1.05)* A	0.967	0.119	0 B	4.11 (0.32) B	2.24 (0.18) B	0.992	0.241	0 B	3.72 (0.23) B	2.47 (0.11) B	0.989	0.208
50.0	0.85 (0.05) A	1.77 (0.05)* A	6.06 (0.19)* A	0.986	0.104	0 B	4.48 (0.34) B	2.15 (0.06) B	0.982	0.183	0 B	4.53 (0.09) B	2.03 (0.22) B	0.991	0.256
52.5	0.81 (0.12)* A	2.24 (0.08)* A	4.92 (0.13)* A	0.994	0.084	0 B	4.49 (0.14) B	2.05 (0.31) B	0.970	0.473	0 B	4.58 (0.39) B	2.01 (0.26) B	0.978	0.377
55.0	0.75 (0.03)* A	3.41 (0.28)* A	3.45 (0.22)* A	0.988	0.212	0 B	4.63 (0.07)* B	1.99 (0.28)* B	0.986	0.350	0 B	4.90 (0.29)* B	1.88 (0.32)* B	0.988	0.320
57.5	0.45 (0.01)* A	5.12 (0.28)*	2.25 (0.06)* A	0.990	0.287	0 B	5.66 (0.29)*	1.63 (0.15)* B	0.994	0.241	0 B	5.82 (0.37)*	1.58 (0.21)* B	0.993	0.276
60.0	0*	8.01 (0.34)*	1.15 (0.07)*	0.990	0.339	0	9.04 (1.16)*	1.02 (0.08)*	0.993	0.321	0	8.91 (0.44)*	1.04 (0.11)*	0.996	0.185

[a] Shown are results for resistance parameters (*Sl*, K_{max}, and time for 4*D*) obtained from the fitting of Geeraerd et al.'s model (24) to the survival curves of the *E. coli* WT and *uvrA* isogenic mutant treated by the UV-H combination in McIlvaine buffer with an absorption coefficient of 23.6 cm^{-1} at different temperatures and recovered in nonselective medium (TSAYE) and selective medium with caffeic acid added (TSAYE-CA). Values in parentheses represent standard deviations of the means. Asterisks indicate significant differences at $P \leq 0.05$ between mean values at treatment temperatures between 40.0 and 60.0°C and those at room temperature in each strain and under each recovery condition. The letters A and B indicate significant differences ($P \leq 0.05$) among mean values of strains recovered in TSAYE medium and the wild-type strain counts obtained in TSAYE-CA medium.

TABLE 3 Heat resistance parameters obtained from the fitting of Geeraerd et al.'s model to the survival curves of the *E. coli* WT strain and its *uvrA* and *recA* isogenic mutants[a]

Temp (°C)	Wild-type strain					*uvrA* mutant					*recA* mutant				
	Sl (min)	K_{max} (min^{-1})	4*D* (min)	R^2	RMSE	*Sl* (min)	K_{max} (min^{-1})	4*D* (min)	R^2	RMSE	*Sl* (min)	K_{max} (min^{-1})	4*D* (min)	R^2	RMSE
55.6	1.13 (0.51) A	0.73 (0.13) A	13.67 (0.95) A	0.988	0.125	2.29 (0.49) A	0.98 (0.07) A	11.76 (0.24) A	0.994	0.075	0 B	1.39 (0.28) B	6.84 (1.52) B	0.976	0.213
58.1	0.61 (0.04) A	2.16 (0.62) A	4.87 (0.15) A	0.991	0.110	0.72 (0.28) A	2.38 (0.73) A	4.58 (1.06) A	0.968	0.177	0 B	4.24 (0.21) B	2.45 (0.36) B	0.976	0.214
60.6	0.27 (0.03) A	7.59 (1.09) A	1.48 (0.02) A	0.982	0.164	0.54 (0.03) A	8.74 (0.07) A	1.60 (0.03) A	0.991	0.129	0 B	10.34 (1.05) B	0.87 (0.13) B	0.982	0.264
63.1	0.11 (0.02) A	20.58 (1.31) A	0.55 (0.03) A	0.996	0.185	0.19 (0.04) A	22.32 (1.46) A	0.60 (0.02) A	0.987	0.163	0 B	23.21 (2.19) A	0.39 (0.05) B	0.985	0.157

[a] Shown are results for the heat resistance parameters (*Sl*, K_{max}, and time for 4*D*) obtained from the fitting of Geeraerd et al.'s model (24) to the survival curves of *E. coli* WT and its *uvrA* and *recA* isogenic mutants treated in McIlvaine buffer at different temperatures and recovered in the nonselective medium. Values in parentheses represent standard deviations of the means. The letters A and B indicate significant differences ($P \leq 0.05$) among mean values of strains at each treatment temperature.

fit. The simultaneous combination of UV light with mild heating significantly improved microbial inactivation. This improvement was explained by the reduction of the *Sl* and the increase of the K_{max} with increasing treatment temperatures (Table 2).

To quantify the contribution of thermal effects to the lethality of the UV-H combined treatment, the heat resistance of the *E. coli* WT was ascertained (Table 3). Figure 2 shows the relationship between treatment temperature and the $\log_{10}$ 4*D* values to heat (thermal death time [TDT] curve) and to UV-H treatments (UV-TDT curve). As expected, the TDT curve obtained for heat treatments showed an exponential course, from which log-linear regression equation was deduced a *z* value of 5.56°C ($R^2 = 0.999$) (representing degrees of temperature increase necessary to reduce the $4D_H$ value 10 times). In contrast, the UV-TDT curve showed a concave downward profile. The lethality of UV-H treatments remained constant below ~45°C, and above this temperature, the lethality increased exponentially, but with a lower thermodependence than heat treatments: The $4D_{UV\text{-}H}$ value would decrease 10 times by increasing the temperature by 12.02°C.

The magnitude of the synergistic lethal effect was calculated by comparing experimental $4D_{UV\text{-}H}$ values with those estimated mathematically (theoretical $4D_{UV\text{-}H}$ values), assuming that the effect of the combined treatment was additive (equation 1). The theoretical UV-TDT curve is also included in Fig. 2 (dotted line), so that the area between the experimental and theoretical UV-TDT curves illustrates the magnitude of the synergistic lethal effect.

Residence time distribution and delivered dose at different temperatures. The RTD curves of the entire installation at 25.0, 50.0, 55.0, and 60.0°C were obtained by the stimulus-response method in a McIlvaine buffer flowing at 8.5 liters h^{-1}. RTD curves were normalized, and the mean residence time ($\bar{t}$) and the variance (σ^2) from the point of tracer injection were obtained. No statistically significant differences ($P > 0.05$) were found among $\bar{t}$ and σ^2 values obtained at 25.0°C ($\bar{t} = 4.36 \pm 0.14$ min, $\sigma^2 = 34.66 \pm 1.69$ min^2), 50.0°C ($\bar{t} = 4.41 \pm 0.09$, $\sigma^2 = 35.10 \pm 5.78$ min^2), 55.0°C ($\bar{t} = 4.31 \pm 0.11$ min, $\sigma^2 = 31.04 \pm 0.77$ min^2), and 60.0°C ($\bar{t} = 4.21 \pm 0.12$ min, $\sigma^2 = 30.23 \pm 2.75$ min^2).

The actinometry iodide-iodate technique was used to study the effect of temperature on the delivered dose. Figure 3 illustrates the absorbance of I_3^- photoproducts induced by UV light in the McIlvaine buffer with an absorption coefficient of 23.6 cm^{-1}. As observed in the figure, the delivered UV dose decreased at temperatures between 50.0 and 60.0°C, the range of treatment temperatures at which the UV susceptibility of the *E. coli* WT increases.

UV resistance of *E. coli* derivatives deficient in DNA repair mechanisms. To study the UV inactivation kinetics of the wild-type strain and its isogenic mutants (Table 1), they were treated in McIlvaine buffer of a low absorption coefficient (15.4 cm^{-1}) and recovered in the nonselective medium (TSAYE) (Fig. 4). As observed in the figure, the $\log_{10}$ values of survivors of *uvrA* and *recA* mutants decreased linearly with the delivered dose. Meanwhile, inactivation curves of *phr*, *nth*, and *umuD* mutants showed an initial shoulder followed by an exponential inactivation phase similar to that of the parental strain. Survival curves were fitted to the model of Geeraerd et al.; the calculated parameters are pre-

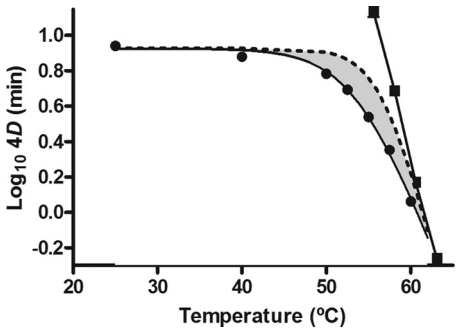

FIG 2 Relationship between treatment temperature and 4*D* values to heat (■) and to UV-H treatments (●) of the *E. coli* WT strain. Experiments were carried out in McIlvaine buffer with an absorption coefficient of 23.6 cm^{-1}, and cells were recovered in the nonselective medium. The figure includes the theoretical UV-TDT (dotted line) calculated by equation 1.

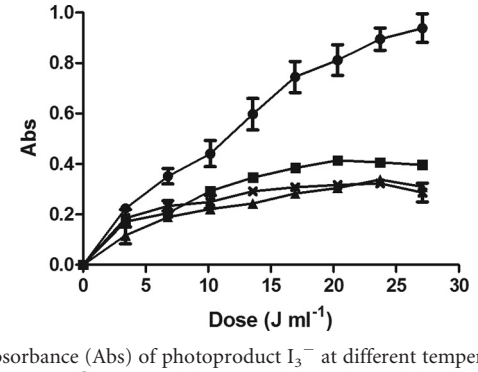

FIG 3 Absorbance (Abs) of photoproduct I_3^- at different temperatures and UV doses: 25.0°C (●), 50.0°C (■), 55.0°C (▲), and 60°C (X). Chemical quantification of the delivered UV intensity was performed with the iodide-iodate actinometer added to buffer of an absorption coefficient of 23.6 cm^{-1}. Determination of photoproduct I_3^- was carried out spectrophotochemically using an extinction coefficient of $\varepsilon_{352} = 27.60$ M^{-1} cm^{-1}.

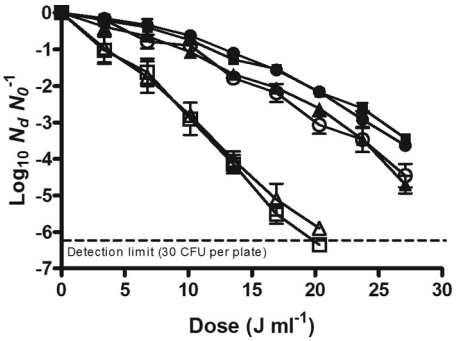

FIG 4 Survival curves of the *E. coli* WT strain (●) and its *nth* (■), *phr* (▲), *umuD* (○), *uvrA* (trio), and *recA* (□) isogenic mutant strains treated by UV light at room temperature in McIlvaine buffer with an absorption coefficient of 15.3 cm^{-1} and recovered in the nonselective medium.

sented in Table 4. No statistically significant differences ($P > 0.05$) were found between the 4*D* values, as well as *Sl* and K_{max} parameters, of the parental strain and the *nth* mutant. The UV sensitivity of the *phr* and *umuD* mutants (4*D* = 26.30 ± 1.15 and 26.77 ± 1.13 J ml^{-1}, respectively) increased slightly compared to that of the parental strain (4*D* = 29.93 ± 1.54 J ml^{-1}), decreasing the shoulder length of the survival curve (Table 4). However, the UV resistance of the *uvrA*- and *recA*-deficient strains diminished drastically (4*D* = 12.21 ± 0.93 and 11.07 ± 0.43 J ml^{-1}, respectively). The concave downward profile of the survival curve of the parental strain became linear in *uvrA* and *recA* mutants (Fig. 4) as the shoulder disappeared; in addition, the inactivation rate almost duplicated. Table 4 also includes the resistance parameters of the wild-type strain treated by UV light at room temperature and recovered in the caffeic acid selective medium (TSAYE-CA) and in the nonselective medium after a photoreactivation step before incubation (TSAYE plus visible light −11.15 klx for 60 min). The photoreactivation process improved the UV survival of *E. coli* WT, increasing the 4*D* value by 17.6%. The parental strain inactivation curve obtained in the TSAYE-CA medium followed a similar profile to those obtained with *uvrA* and *recA* mutant cells in TSAYE (Fig. 4): the shoulder disappeared, and the inactivation rate increased (Table 4). In fact, there were no statistically significant differences ($P > 0.05$) among the mean 4*D* values of the parental strain recovered in TSAYE-CA (12.37 ± 0.32 J ml^{-1}) and those of its *uvrA* and *recA* mutant derivatives recovered in TSAYE. Similar results were obtained with buffer with a high absorption coefficient (data not shown).

Heat resistance characterization of *uvrA* and *recA* mutants. The heat resistance characterization of the two most UV-sensitive *E. coli* derivatives (*uvrA* and *recA* mutants) was performed (Table 3). The data of Table 3 show that heat survival curves of the *uvrA* mutant had long shoulders, like the parental strain, whereas shoulders were not present in the *recA* mutant. Moreover, 4*D* values obtained from the *recA* mutant were about half of those obtained for the parental strain and for the *uvrA* mutant at all temperatures tested. As the *uvrA* mutant showed the same heat resistance as the wild-type strain, it was chosen for further studies.

UV-H resistance of the *uvrA* mutant and the wild-type strain recovered in nonselective and caffeic acid selective medium. Resistance parameters of the *uvrA*-deficient microorganism recovered in the nonselective medium and its isogenic wild-type strain, also recovered in the caffeic acid-supplemented medium, are shown in Table 2. As observed in the table, the survival curves of the *uvrA* mutant recovered in TSAYE and those of the parental strain recovered in TSAYE-CA did not show shoulders, and no statistically significant differences ($P > 0.05$) were found between their K_{max} values at all temperatures tested. A comparison of the 4*D* values of the *uvrA* mutant with those of the parental strain recovered in the nonselective medium shows that the former was significantly less UV-H resistant. However, this difference in resistance was reduced by increasing the treatment temperature. This phenomenon is also illustrated in Fig. 5, where the experimental UV-TDT curves of the *uvrA* mutant and of the parental strain are plotted. For the mutant strain, the lethal contribution of heat was not observed at temperatures below ~55°C, and above this temperature, the lethality increased with a similar thermodependence to heat treatments. In addition, the experimental and theoretical UV-TDT curves of the *uvrA* mutant overlapped (Fig. 5), which means that no synergistic lethal effect occurred, contrary to that observed for the parental strain (Fig. 2).

Role of membrane fluidity on the UV-H resistance of *E. coli*. Figure 6 shows the percentage of decrease of DPH fluorescence anisotropy in the *E. coli* WT and *uvrA* mutant membrane after

TABLE 4 UV resistance parameters obtained from the fitting of Geeraerd et al.'s model to the survival curves of the *E. coli* WT strain and its *nth*, *phr*, *umuD*, *uvrA*, and *recA* isogenic mutants[a]

Derivative	Recovery medium	*Sl* (J ml^{-1})	K_{max} (ml J^{-1})	4*D* (J ml^{-1})	R^2	RMSE
WT	TSAYE	8.78 (0.20) A	0.44 (0.03) A	29.93 (1.54) A	0.989	0.145
	TSAYE-visible light	10.05 (1.50) A	0.36 (0.08) A	35.19 (1.28) B	0.938	0.254
	TSAYE-CA	0 B	0.80 (0.05) B	12.37 (0.32) C	0.986	0.368
Mutant						
nth	TSAYE	6.95 (0.44) A	0.42 (0.02) A	28.54 (1.50) A	0.969	0.196
phr	TSAYE	6.84 (1.11) C	0.47 (0.05) A	26.30 (1.15) D	0.977	0.269
umuD	TSAYE	5.95 (1.56) C	0.46 (0.08) A	26.77 (1.13) D	0.984	0.208
uvrA	TSAYE	0 B	0.77 (0.05) B	12.21 (0.93) C	0.992	0.271
recA	TSAYE	0 B	0.79 (0.01) B	11.07 (0.43) C	0.986	0.372

[a] Shown are the results for UV resistance parameters (*Sl*, K_{max}, and dose for 4*D*) obtained from the fitting of Geeraerd et al.'s model (24) to the survival curves of *E. coli* WT and its *nth*, *phr*, *umuD*, *uvrA*, and *recA* isogenic mutants in McIlvaine buffer with an absorption coefficient of 15.3 cm^{-1} at room temperature. The table includes resistance parameters of the wild-type strain recovered in nonselective medium (TSAYE) and selective medium with caffeic acid added (TSAYE-CA) and with a previous photoreactivation step before incubation (TSAYE-visible light [11.15 klx for 60 min]).Values in parentheses represent standard deviations of the means. The letters A, B, C, and D indicate significant differences ($P \leq 0.05$) between values of the wild-type strain recovered under different conditions and its derivatives recovered in TSAYE.

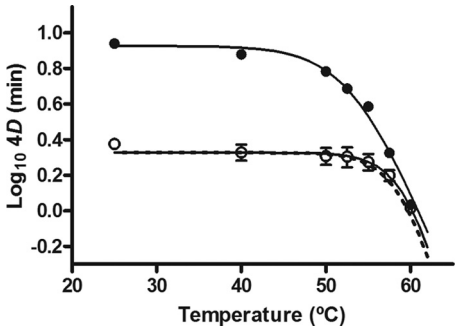

FIG 5 UV-TDT (4*D*) curves of the *E. coli* WT strain (●) and the *uvrA* mutant (○). UV-H treatments were carried out in McIlvaine buffer with an absorption coefficient of 23.6 cm^{-1}, and both strains were recovered in nonselective medium. The figure includes the theoretical UV-TDT curve (dotted line) of the *uvrA* mutant calculated by equation 1.

cells were maintained for 3.5 min at temperatures between 25.0 and 58.0°C. The percentage of synergism previously calculated for UV-H treatments of the *E. coli* WT (equation 2) has also been included (dotted line) for comparison. The decrease of DPH fluorescence anisotropy with temperature in the *E. coli* WT and *uvrA* mutant membranes showed the same tendency. The fluidity of the membrane of *E. coli* remained constant as the temperature increased to approximately 40 to 45°C. Further increases in temperature caused a decrease in DPH fluorescence anisotropy, which indicates an increase in membrane fluidity. This profile reflected the curve corresponding to the percentage of synergism (Fig. 6), which started to be relevant at temperatures of ~40 to 45°C and increased steadily up to 55°C. Further increases in temperature did not induce higher UV-H synergistic lethal effects due to the predominance of heat lethality over the lethal effects of the UV light. These results suggested that the fluidification of the membrane could contribute to the synergistic lethal effect of UV-H treatments.

To test this hypothesis, the *E. coli* WT and the *uvrA* mutant were treated by UV light at room temperature after induction of its membrane fluidification with benzyl alcohol (BA). BA has been widely used to investigate the correlation between membrane fluidity and membrane function because it is able to induce physical

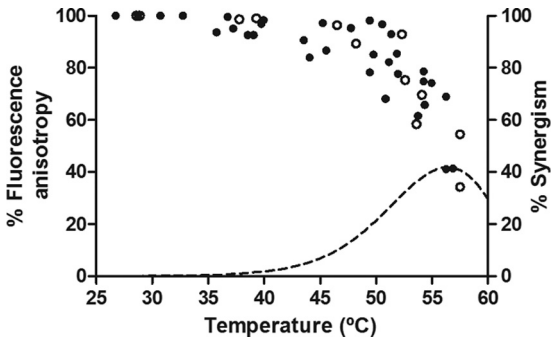

FIG 6 Percentage of DPH fluorescence anisotropy changes in the *E. coli* WT strain (solid symbols) and *uvrA* mutant (open symbols) membrane at different temperatures. Cells were treated for 3.5 min in McIlvaine buffer at temperatures of between 25.0 and 60.0°C. The figure includes the percentage of synergism of UV-H treatments at different temperatures of the *E. coli* WT strain (dotted line) calculated by equation 2.

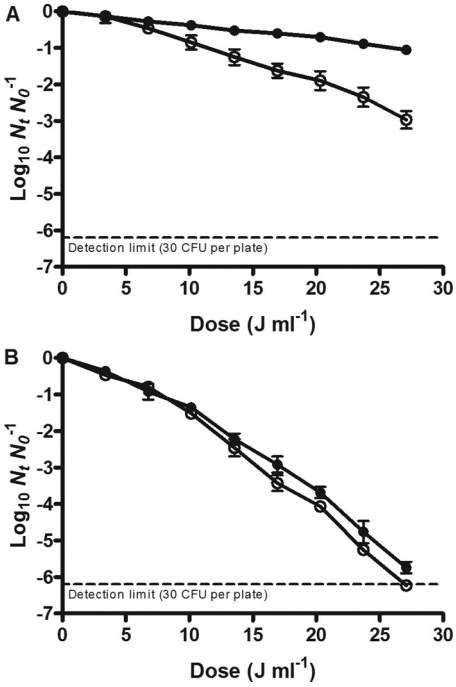

FIG 7 Survival curves of the *E. coli* WT strain (A) and its *uvrA* isogenic mutant (B) to UV light at room temperature in McIlvaine buffer with an absorption coefficient of 23.6 cm^{-1} with (open symbols) and without (solid symbols) benzyl alcohol. Cells were recovered in the nonselective medium.

membrane disorders without impairing cell viability (28). Before treatments, cells were incubated in the McIlvaine buffer with 20 mM BA added for 20 min. This treatment triggered a decrease of 30 to 40% of DPH fluorescence anisotropy in the parental strain and in the *uvrA* mutant strains, indicating a fluidification of the membrane (data not shown). The survival curves of the BA-exposed cells of the parental strain and the *uvrA* mutant strains against UV treatments (23.6 cm^{-1}) are represented in Fig. 7. As can be observed in the figure, the UV resistance of the parental strain was significantly reduced (decrease in 4*D* values from 64.62 ± 2.86 J ml^{-1} to 29.52 ± 1.52 J ml^{-1}) when cells had been previously exposed to BA. However, membrane fluidification in the *uvrA* mutant did not change its UV resistance ($P > 0.05$).

DISCUSSION

The present results show that the UV susceptibility of *E. coli* WT was augmented with increasing treatment temperatures (Fig. 1 and Table 2). This sensitization was due to a decrease of the shoulder length and an increase of the inactivation rate. Shoulder length has been related to damage repair capacity (12, 16); therefore, shorter shoulders at higher temperatures could be due to a reduction in cellular capacity to repair damage or to the appearance of additional lethal damage that arises from the interaction of lesions induced by both agents.

The relationship between treatment temperature and the $\log_{10}$ 4*D* values of the UV-H treatments (UV-TDT curve) showed a concave downward profile (Fig. 2). Accordingly, the UV lethality of the *E. coli* WT did not change by increasing the temperature to ~45°C, and above this temperature, it was exponentially augmented at a rate of 10-fold for each temperature increase of 12.02°C. The theoretical 4*D* values of UV-H treatments were cal-

culated assuming that the lethal effect of the combined treatment was additive (equation 1) and are plotted in Fig. 2 (theoretical UV-TDT curve). There was a range of temperatures at which theoretical 4*D* values were higher than experimental values, from which it was deduced that there was a synergistic lethal effect. The area between experimental and theoretical UV-TDT curves illustrates the evolution of the magnitude of the synergism. The maximum synergistic lethal effect of all tested temperatures was found at 55.0°C (40.3% of synergism), a temperature value that was similar to that reported for *E. coli* STCC 4201 (12) and *Salmonella* Typhimurium (16). Above 55°C, the synergistic lethal effect decreased. This was probably due to the higher heat dependence of the thermal inactivation ($z = 5.56$°C) compared to UV-H inactivation ($z = 12.02$°C). The faster increase with temperature of the thermal lethality would finally make the lethality of UV negligible, and therefore the 4*D* values for both technologies become the same. It would be also possible that above 55°C, changes may occur in some cellular components that would lead to a reduction in the synergistic effect.

Temperature affects the rheological properties of liquids and consequently modifies the flow behavior and the velocity profile of flowing liquids (29); therefore, it can influence the residence time distribution. As a first step, we observed that increasing the temperature between 25.0 and 60.0°C did not change the flow pattern under our experimental conditions ($\bar{t} = 4.36 \pm 0.14$ min and $\sigma^2 = 34.66 \pm 1.69$ min^2 and $\bar{t} = 4.21 \pm 0.12$ min and $\sigma^2 = 30.23 \pm 2.75$ min^2, respectively). Therefore, the synergistic lethal effect was not due to rheological changes. On the other hand, the dose delivered by UV lamps could change with temperature and could perhaps explain the increase of UV-H lethality at higher temperatures. However, the results demonstrated that the delivered dose that reached the treatment medium was reduced between 50.0 and 60.0°C (Fig. 3), coinciding with the temperature range in which UV-H lethality increased. These results are consistent with the fact that the production of 254-nm UV irradiation by low-pressure lamps increases with respect to ambient temperature up to a maximum level at 40°C and then drops with increasing temperature (6). Thus, the change of the delivered dose emitted by lamps does not explain the synergistic lethal effect. Overall, we conclude that no photophysical effect contributed to the observed synergism of the combined UV-H process, and it should therefore be explained through its biological effects.

The synergistic lethality of UV-H treatments could be due to an improvement of the UV effects on the DNA molecule, either through interference with DNA repair mechanisms or through an increase of the damage to the DNA. To evaluate the effect of the combined UV-H process on *E. coli*'s DNA repair capacity, we used derivative strains deficient in different repair mechanisms. According to our results (Fig. 4 and Table 4), the microorganism carrying the *nth* mutation exhibited the same degree of UV sensitivity as the wild-type strain, which indicates that base excision repair mediated by the thymine glycol DNA (TG-DNA) glycosylase would not intervene in the UV-C resistance of *E. coli*. This finding was not surprising since TG-DNA glycosylase is involved in the repair of DNA oxidative damage (5-hydroxycytosine, urea, and thymine glycol lesions) (3), induced primarily at higher UV wavelengths (UV-A and UV-B) (30) than those used in this study. The deletion of the *umuD* gene, essential to construct polymerase V, which is involved in the translesion synthesis pathway (5), scarcely increased UV cell sensitivity. On the other hand, the deletion of the *phr* gene also resulted in a slight increase in *E. coli* UV sensitivity (17.6% after a photoreactivation step). Sancar et al. (31) demonstrated that DNA photolyase may interact with CPD lesions, facilitating the incision of the UvrABC exinuclease. Strains harboring mutations in one of the *uvr* loci (*uvrA*, *uvrB*, or *uvrC*) are unable to remove thymine dimers by nucleotide excision repair, failing to survive even a small UV dose (32). Accordingly, the UV survival curve obtained with the parental strain recovered in medium with caffeic acid added produced the same pattern as the *uvrA* mutant (Table 4). RecA nucleofilament protein is directly involved in the implementation of SOS response repair mechanisms (5). The *recA* mutant showed the same degree of UV sensitivity as the *uvrA* strain. All of these results taken together indicate that the factors most relevant to UV-C survival in the *E. coli* WT strain are UvrABC-mediated nucleotide excision repair and RecA-dependent repair systems. Given the coincidence among survival curves of the *recA* and the *uvrA* mutants, it is also feasible that the loss of UV resistance in both strains is due to a defect in the same repair pathway, which would be nucleotide excision repair mediated by RecA protein (RAMER). This hypothesis agrees with the results of Bichara et al. (33).

The heat resistance characterization of the most UV-sensitive mutants (*uvrA* and *recA* mutants) showed that the *recA* mutant was more sensitive to heat treatments since 4*D* values were approximately half of those corresponding to the parental strain at all temperatures tested (Table 3), indicating that the RecA protein is also involved in cellular protection from heat. The *E. coli uvrA* mutant was considered the most appropriate derivative strain to continue our investigation due to its defect in DNA damage repair and its similarity in heat tolerance to the parental strain. Subsequently, determination of the UV-H resistance at different temperatures of the strain carrying the *uvrA* mutation was performed. The UV-TDT curve of the *uvrA* mutant showed, like the parental strain, a downward concave profile (Fig. 5). However, its experimental UV-TDT curve overlapped with the theoretical curve, confirming that the UV-H treatments of the *uvrA* mutant did not exhibit a synergistic lethal effect. Moreover, the resistance parameters of the *uvrA* mutant recovered in the nonselective medium and the wild-type strain recovered in the caffeic acid-supplemented medium were similar (Table 2). Therefore, it can be concluded that the synergistic lethal effect observed in UV-H treatments was due to the inhibition of DNA excision repair mechanisms by the action of heat and not to a higher degree of direct DNA damage as previously suggested.

This phenomenon may explain the inactivation of UV-H kinetics. The UV-H survival curves of the wild-type strain (Fig. 2) showed initial shoulder phases, which decreased with increasing treatment temperature, followed by an exponential order of death. The shoulder phases obtained under our experimental conditions can be attributed to the action of DNA repair mechanisms, given the lack of the lag phase in the UV survival curves of the *uvrA* and *recA* mutant derivatives and in the survival curves of the parental strain in the presence of caffeic acid, which prevents UvrABC action.

Finally, the motivation behind inhibiting the excision repair pathway requires clarification. The idea that heat could induce conformational and structural changes in UvrABC proteins inhibiting its enzymatic activity was immediately discarded since, as we have reported before (16), the application of a heat treatment before the UV treatment did not increase the UV susceptibility of

Salmonella Typhimurium, merely showing an additive lethal effect. Geveke (13) suggested that the UV-H synergistic lethal effect observed in *E. coli* treated in egg whites (30 to 50°C) could be related to changes in the physical state of the cell membrane induced by heat. This hypothesis may be consistent with our results since the incision steps of UvrABC and RecA activity during SOS are reportedly associated with the inner membrane of *E. coli* (34). Moreover, Todo et al. (35) demonstrated, using an unsaturated fatty acid auxotroph of *E. coli*, that the fluidification state of cell membranes influences the recovery of UV-irradiated cells. Hence, we proceeded to determine the membrane fluidity changes induced by heating. The relationship between the DPH fluorescence anisotropy decreased in the *E. coli* WT and *uvrA* mutant, and the treatment temperature showed a similar profile to the experimental UV-TDT curves of both strains (Fig. 6). Both the thermal fluidification of membranes and the synergistic lethal effects of *E. coli* WT started around 40 to 45°C. In addition, the incubation of *E. coli* cells in the treatment medium with the membrane-fluidizing agent BA reduced the UV resistance of the parental strain, whereas it did not change the UV resistance of the *uvrA* mutant strain (Fig. 7). These results indicate that the physical state of the membrane during treatment in the parental strain of *E. coli* (i.e., its fluidity) influenced its UV resistance. Cells with a more fluid membrane were more sensitive to the action of UV, and this increase in fluidity upon heating may explain the synergistic lethal effect observed in UV-H treatments applied to the parental strain. Since this effect did not occur in the *uvrA* mutant strain, we have to assume that the decrease in survival caused by membrane fluidization is linked to the poor functioning of the nucleotide excision repair mechanisms in the parental strain.

In conclusion, the results obtained in this investigation demonstrate that the synergistic lethal effect of UV-H treatments in *E. coli* resulted from the inhibition of DNA excision repair due to membrane fluidification caused by simultaneous heating. Thus, UV-induced DNA lesions remained unrepaired, decreasing *E. coli*'s UV survival. This raises the possibility of combining fluidizing membrane agents with UV light treatments to improve UV light's lethality in, for example, food processing applications.

ACKNOWLEDGMENTS

This study was carried out with financial support from the Ministerio de Ciencia e Innovación, EU-FEDER (CIT020000-2009-40) and the Departamento de Ciencia, Tecnología y Universidad del Gobierno de Aragón. E.G. gratefully acknowledges the financial support for her doctoral studies provided by the Ministerio de Educación y Ciencia.

REFERENCES

1. **Hijnen WAM, Beerendonk EF, Medema GJ.** 2006. Inactivation credit of UV radiation for viruses, bacteria and protozoan (oo)cysts in water: a review. Water Res. **40:**3–22.
2. **Guerrero-Beltrán JA, Barbosa-Cánovas GV.** 2004. Advantages and limitations on processing foods by UV light. Food Sci. Technol. Int. **10:**137–147.
3. **Sinha RP, Hader DP.** 2002. UV-induced DNA damage and repair: a review. Photochem. Photobiol. Sci. **1:**225–236.
4. **Friedberg EC, Walker GC, Siede W, Wood RD, Schultz RA, Ellenberger T.** 2006. DNA repair and mutagenesis, 2nd ed. ASM Press, Washington, DC.
5. **Bichara M, Meier M, Wagner J, Cordonnier A, Lambert IB.** 2011. Postreplication repair mechanisms in the presence of DNA adducts in *Escherichia coli.* Mutat. Res. Rev. Genet. **727:**104–122.
6. **Koutchma T, Forney LJ, Moraru CL.** 2009. Ultraviolet light in food technology. CRC Press, Boca Raton, FL.
7. **USFDA.** 2000. Irradiation in the production, processing and handling of food. Fed. Regist. **65:**71056–71058.
8. **Ha JH, Ha SD.** 2011. Synergistic effects of sodium hypochlorite and ultraviolet radiation in reducing the levels of selected foodborne pathogenic bacteria. Foodborne Pathog. Dis. **8:**587–591.
9. **Rincon AG, Pulgarin C.** 2004. Bactericidal action of illuminated TiO_2 on pure *Escherichia coli* and natural bacterial consortia: post-irradiation events in the dark and assessment of the effective disinfection time. Appl. Catal. B Environ. **49:**99–112.
10. **Koivunen J, Heinonen-Tanski H.** 2005. Inactivation of enteric microorganisms with chemical disinfectants, UV irradiation and combined chemical/UV treatments. Water Res. **39:**1519–1526.
11. **Petin VG, Morozov II, Kim JK, Semkina MA.** 2011. Quantitative estimation of UV light dose concomitant to ionizing irradiation. Radiats. Biol. Radioecol. **80:**33–37. (In Russian.)
12. **Gayán E, Monfort S, Alvarez I, Condón S.** 2011. UV-C inactivation of *Escherichia coli* at different temperatures. Innov. Food Sci. Emerg. Techno. **12:**531–541.
13. **Geveke DJ.** 2008. UV inactivation of *E. coli* in liquid egg white. Food Bioprocess Technol. **1:**201–206.
14. **Petin VG, Zhurakovskaya GP, Komarova LN.** 1997. Fluence rate as a determinant of synergistic interaction under simultaneous action of UV light and mild heat in *Saccharomyces cerevisiae.* J. Photochem. Photobiol. B **38:**123–128.
15. **Gayán E, Serrano MJ, Monfort S, Alvarez I, Condón S.** 2012. Combining ultraviolet light and mild temperatures for the inactivation of *Escherichia coli* in orange juice. J. Food Eng. **113:**598–605.
16. **Gayán E, Serrano MJ, Raso J, Alvarez I, Condón S.** 2012. Inactivation of *Salmonella enterica* by UV-C light alone and in combination with mild temperatures. Appl. Environ. Microbiol. **78:**8353–8361.
17. **Baba T, Ara T, Hasegawa M, Takai Y, Okumura Y, Baba M, Datsenko KA, Tomita M, Wanner BL, Mori H.** 2006. Construction of *Escherichia coli* K-12 in-frame, single-gene knockout mutants: the Keio collection. Mol. Syst. Biol. **2:**2006.02008. doi:10.1038/msb4100050.
18. **Dawson RMC, Elliot DC, Elliot WH, Jones KM.** 1974. pH, buffers and physiological media, p 484–485. *In* Dawson RMC, Elliot DC, Elliot WH, Jones KM (ed), Data for biochemical research, 2nd ed. Clarendon Press, Oxford, United Kingdom.
19. **Condón S, Arrizubieta MJ, Sala FJ.** 1993. Microbial heat resistance determinations by the multipoint system with the thermoresistometer TR-SC: improvement of this methodology. J. Microbiol. Methods **18:**357–366.
20. **Fong K, Bockrath RC.** 1979. Inhibition of deoxyribonucleic-acid repair in *Escherichia-coli* by caffeine and acriflavine after ultraviolet-irradiation. J. Bacteriol. **139:**671–674.
21. **Selby CP, Sancar A.** 1991. Noncovalent drug-DNA binding interactions that inhibit and stimulate (A)BC excinuclease. Biochemistry **30:**3841–3849.
22. **Condón S, Oria R, Sala Trepat FJ.** 1987. Heat resistance of microorganisms: an improved method for survival counting. J. Microbiol. Methods **7:**37–44.
23. **Geeraerd AH, Valdramidis VP, Van Impe JF.** 2005. GInaFiT, a freeware tool to assess non-log-linear microbial survivor curves. Int. J. Food Microbiol. **102:**95–105.
24. **Geeraerd AH, Herremans CH, Van Impe JF.** 2000. Structural model requirements to describe microbial inactivation during a mild heat treatment. Int. J. Food Microbiol. **59:**185–209.
25. **Almeida LM, Vaz WC, Zachariasse KA, Madeira VMC.** 1982. Fluidity of sarcoplasmic-reticulum membranes investigated with dipyrenylpropane, an intramolecular excimer probe. Biochemistry **21:**5972–5977.
26. **Chu-Ky S, Tourdot-Marechal R, Marechal Guzzo P-AJ.** 2005. Combined cold, acid, ethanol shocks in *Oenococcus oeni*: effects on membrane fluidity and cell viability. Biochim. Biophys. Acta **1717:**118–124.
27. **Koutchma T, Parisi B.** 2004. Biodosimetry inactivation in of *Escherichia coli* UV model juices with regard to dose distribution in annular UV reactors. J. Food Sci. **69:**E14–E22.
28. **Shigapova N, Tökrök Z, Balogh G, Goloubinoff P, Vígh L, Horváth I.** 2005. Membrane fluidization triggers membrane remodeling which affects the thermotolerance in *Escherichia coli.* Biochem. Biophys. Res. Commun. **328:**1216–1223.
29. **Torres AP, Oliveira FAR, Fortuna SP.** 1998. Residence time distribution of liquids in a continuous tubular thermal processing system. Part I. Relating RTD to processing conditions. J. Food Eng. **35:**147–163.

30. **Ravanat J-L, Douki T, Cadet J.** 2001. Direct and indirect effects of UV radiation on DNA and its components. J. Photochem. Photobiol. B **63:** 88–102.
31. **Sancar A, Franklin K, Sancar G.** 1984. *Escherichia-coli* DNA photolyase stimulates UvrABC excision nuclease in vitro. Proc. Natl. Acad. Sci. U. S. A. **81:**7397–7401.
32. **Sancar A.** 1996. DNA excision repair. Annu. Rev. Biochem. **65:**43–81.
33. **Bichara M, Pinet I, Lambert LB, Fuchs RPR.** 2007. RecA-mediated excision repair: a novel mechanism for repairing DNA lesions at sites of arrested DNA synthesis. Mol. Microbiol. **65:**218–229.
34. **Lin CLG, Kovalsky O, Grossman L.** 1997. DNA damage-dependent recruitment of nucleotide excision repair and transcription proteins to *Escherichia coli* inner membranes. Nucleic Acids Res. **25:**3151–3158.
35. **Todo T, Yonei S, Kato M.** 1983. The modulating influence of the fluidity of cell-membrane of excision repiar of DNA in UV-irradiated *Escherichia-coli.* Biochem. Biophys. Res. Commun. **110:**609–615.